Published in final edited form as:
J Immunol. 2013 August 1; 191(3): 1453–1464. doi:10.4049/jimmunol.1203318.

Pulmonary expression of Oncostatin M (OSM) promotes inducible-BALT formation independently of IL-6, despite a role for IL-6 in OSM-driven pulmonary inflammation[6]

Fernando M Botelho[1,4], **Javier Rangel-Moreno**[3], **Dominik Fritz**[2], **Troy D Randall**[3,5], **Zhou Xing**[1], and **Carl D Richards**[1]

[1]McMaster Immunology Research Centre, Department of Pathology and Molecular Medicine, Rochester, New York, USA

[2]CIHR Matrix Dynamics Group, University of Toronto, Rochester, New York, USA

[3]Department of Medicine, Division of Allergy Immunology and Rheumatology, University of Rochester Medical Center, Rochester, New York, USA

[4]Department of Immunology and Microbiology, College of Veterinary Medicine, Cornell University, Ithaca, New York, USA

[5]Division of Clinical Immunology and Rheumatology, University of Alabama at Birmingham, Birmingham, Alabama, USA

Abstract

Inducible Bronchus-Associated Lymphoid Tissue (iBALT) is associated with immune responses to respiratory infections as well as with local pathology derived from chronic inflammatory lung diseases. Here we assessed the role of Oncostatin M (OSM) in B cell activation and iBALT formation in mouse lungs. We found that C57Bl/6 mice responded to an endotracheally-administered adenovirus vector expressing mouse OSM (Ad-mOSM), with marked iBALT formation, increased cytokine (IL-4, IL-5, IL-6, IL-10, TNFα and IL-12) and chemokine (CXCL13, CCL20, CCL21, Eotaxin-2, KC and MCP-1) production as well as inflammatory cell accumulation in the airways. B cells, T cells and dendritic cells were also recruited to the lung, where many displayed an activated phenotype. Mice treated with control adenovirus vector (Addl70) were not affected. Interestingly, IL-6 was required for inflammatory responses in the airways and for the expression of most cytokines and chemokines. However, iBALT formation and lymphocyte recruitment to the lung tissue occurred independently of IL-6 and STAT6 as assessed in gene-deficient mice. Collectively, these results support the ability of OSM to induce B cell activation and iBALT formation independently of IL-6 and highlight a role for IL-6 downstream of OSM in the induction of pulmonary inflammation.

[6]This work was funded by the Canadian Institutes for Health Research grant 102562 to CDR and by NIH grant HL069409 to TDR. JRM was supported by start up funds from the department of Medicine, University of Rochester and AI91036.

Corresponding Author: Carl D. Richards, PhD, McMaster University, MDCL-4017, Department of Pathology and Molecular Medicine, 1280 Main Street West, Hamilton, Ontario L8S 4K1 Canada, Phone: 905 525 9140 x22472, Fax: 905 522 6750, richards@mcmaster.ca.

Keywords

Oncostatin M; interleukin-6; lung; iBALT

Introduction

The gp130 family of cytokines, including IL-6, IL-11, LIF, IL-31 and Oncostatin M (OSM) play various roles in inflammation, hematopoiesis and immune responses (1,2). Receptors for this family of cytokines share a common subunit, gp130, which complexes with a variety of cell surface and soluble receptor chains that provide specificity for the separate ligands (2). Functions of this family of cytokines in mucosal immunity are complex and overlapping due to the combinatorial expression of shared and specific receptor subunits on various cell types. Previous studies indicate shared but also private and specific activities of OSM among gp130 cytokines (2,3). However, the regulatory roles of OSM in lung mucosal immunity are currently unclear.

OSM is a 26kDa extracellular pro-inflammatory glycoprotein that promotes connective tissue remodeling, chemokine expression and infiltration of inflammatory granulocytes, lymphocytes and myeloid cells in animal models (4-8). Lung OSM levels are elevated in patients with severe asthma (9), allergic rhinitis (10) and idiopathic pulmonary fibrosis (IPF) (11). Inflammatory mononuclear cells are a major source of OSM (12), while its specific receptors, consisting of gp130 and an OSM-specific receptor-beta subunit (3) are broadly expressed by structural cells, such as fibroblasts, osteoblasts, smooth muscles cells and endothelial cells.

Although the effects of OSM on structural cells in various systems have been described, fewer studies have examined its effects on hematopoietic immune cells. Activated myeloid- and lymphoid cells secrete OSM (3, 12) and the presence of mononuclear cells producing OSM *in vivo* correlates with neutrophil influx during early stages of inflammation (13). Additionally, myeloid dendritic cells (DCs) express OSM receptors and respond to OSM by differentiating into potent antigen-presenting cells (14). Transgenic over-expression of OSM stimulates extrathymic T cell differentiation, expansion of memory T cells (15), accumulation of immature B cells and production of circulating auto-antibodies (16).

The prototype gp130 family member: IL-6 has effects on ectopic lymphoid tissue development in rodent lungs. IL-6 over-expression (along with the IL-6R) promotes the formation of inducible Bronchus-Associated Lymphoid Tissue (iBALT) (17), a tertiary lymphoid structure that contains large B cell aggregates, surrounded by T cells and maintained by DCs (18,19). Working together with classical lymphoid tissues, iBALT helps control respiratory pathogens (20). The presence of iBALT is associated with various lung inflammatory conditions, including severe asthma, COPD (18) and lung complications of rheumatoid arthritis (21). iBALT has been detected in the lungs of mice infected with virus (20), mycobacteria (22) or exposed neonatally to the bacterial product lipopolysaccharide (LPS) (23), although the precise pathways by which each of these conditions result in iBALT might not be identical (24). In any case, the function of OSM in iBALT formation and B cell responses during respiratory infection remains to be understood.

Here, we examined the role of OSM in iBALT formation and activation of B cell lymphocyte populations using an adenoviral vector expressing murine OSM (Ad-mOSM). This approach allows us to investigate transient OSM transgenic expression in the context of viral infection in mouse lungs. Since OSM has been demonstrated to markedly induce IL-6 expression (25), we further assessed the biological effects of Ad-mOSM and control vectors in wild-type C57BL/6 (WT) and *IL-6*$^{-/-}$ mice. We observed that Ad-mOSM induced significant inflammation, B cell activation and iBALT formation, particularly in the lung parenchyma. While inflammation in the airways was markedly reduced in *IL6*$^{-/-}$ mice, B cell accumulation, activation and iBALT formation in the lung tissue was independent of IL-6.

Materials and Methods

Animals

C57BL/6 (WT) and IL-6-deficient mice (IL-6$^{-/-}$, C57Bl/6 background, 6-8 weeks old) were purchased from The Jackson Laboratories (Bar Harbor, ME, USA). Mice were maintained under specific pathogen-free conditions in an access-restricted area, on a 12h light-dark cycle, with food and water provided *ad libitum*. The Animal Research Ethics Board of McMaster University approved all experiments. Endo-tracheal administration of indicated amounts (PFU) of control adenovirus vector (Addel70) or vector expressing mouse OSM (Ad-mOSM) has been previously described (25).

Bronchoalveolar lavage

Bronchoalveolar lavage (BAL) fluid was collected after instilling lungs with 0.4 ml of ice-cold phosphate-buffered saline (PBS (Invitrogen, Carlsbad, California)) twice. Total cell numbers were determined using a haemocytometer. BAL cytospins were prepared for differential cell counts and stained with Hema-3 (Biochemical Sciences Inc., Swedesboro, New Jersey, USA). 500 cells in each cytospin slide were examined to identify and count macrophages, lymphocytes, neutrophils and eosinophils. To detect cytokine levels in BAL samples (stored at -80°C before use), ELISA (purchased from R&D Systems Inc) and Luminex bead assays were used according to the protocol recommended by the manufacturer.

Isolation of lung mononuclear cells and flow cytometric analysis

Lung mononuclear cell suspensions were generated by mechanical mincing and collagenase digestion. Debris were removed by passage through 45 micrometer screen size nylon mesh and cells were resuspended in PBS containing 0.3% bovine serum albumin (BSA) (Invitrogen, Burlington, ON, Canada) or in RPMI supplemented with 10% fetal bovine serum (FBS) (Sigma-Aldrich, Oakville, ON, Canada), 1% L-glutamine, and 1% penicillin/streptomycin (Invitrogen, Burlington, ON, Canada). 1×10^6 lung mononuclear cells were washed once with PBS/0.3% BSA and stained with primary antibodies directly conjugated to fluorochromes for 30 minutes at 4°C. 10^5 live events were acquired on an LSR II (BD Biosciences, San Jose, California) flow cytometer and the data were analyzed with FlowJo analysis software (TreeStar Inc., Ashland, Oregon). Side scatter-, and forward scatter parameters internalization of 7-aminoactinomycin D (eBiosciences; San Jose, California) by dead cells were used to define live cell and lymphocyte gates. All antibodies were purchased

from BD Biosciences (San Jose, California) or eBiosciences (San Diego, California) unless otherwise stated. The following antibodies were used for flow cytometric analysis: PE-cy5-conjugated anti-CD69, PerCP-cy5.5-conjugated anti-CD11c, APC-conjugated anti-MHC class II, Alexa Fluor 700-conjugated anti-CD86, APC-cy7-conjugated anti-CD45, and Pacific Blue-conjugated anti-CD3. Qdot605-conjugated anti-CD4 and Qdot655-conjugated anti-B220 were purchased from Invitrogen (Carlsbad, California). V500-conjugated anti-CD8 was purchased from BD Biosciences (San Jose, California).

Histological analysis and immunofluorescence staining of iBALT

The entire lung was fixed at 30 cm H_20 pressure in 10% formalin for histological assessment. Lungs were embedded in paraffin blocks and 4-μm-thick cross-sections were cut and stained with hematoxylin and eosin (H&E) to assess lung inflammation. Immunofluorescent staining was performed as previously described (26). For immunofluorescence analyses, slides were hydrated in PBS and blocked for 30 min at 25°C with F_c Block (10 μg/ml) and 5% (vol/vol) normal donkey serum in PBS. Endogenous biotin was blocked with a sequential avidin-biotin incubation step (Sigma-Aldrich). After blockade, the slides were incubated overnight at 25°C with rat anti-B220 (clone RA3-6B2. BD Pharmingen) to visualize B cells, anti-CD21-CD35 (clone 7E9, Biolegend, San Diego, CA) in combination with rat anti mouse follicular dendritic cell (clone FDCM1, BD Pharmingen) to detect follicular dendritic cells (FDC), goat anti-CD3ε to stain T cells (clone M-20, Santa Cruz Biotechnology, CA), goat anti-PCNA from Santa Cruz Biotechnology Inc (clone C-20, Santa Cruz, CA) to detect proliferating cells and peanut agglutinin (L7381, SIGMA) to detect germinal center B cells (GC B cells). Fluorescently labeled secondary antibodies were incubated for 3h at room temperature. Finally, the slides were incubated with streptavidin conjugated to either Alexa Fluor 594 or Alexa Fluor 488 and counterstained with ProLong Gold anti-fade with DAPI from Invitrogen. All sections were viewed with a Zeiss Axioplan 2 microscope. Images were recorded with a Zeiss AxioCam HR digital camera.

Neutralizing Antibody Assay

Frozen serum samples were used to determine the neutralizing antibody (Ab) titre. Serial dilutions of sera were added to Ad–LacZ and the ability of serum antibodies to block the infection of Hela cells with Ad-LacZ was evaluated with a colorimetric assay 24 hours after infection. The titre is expressed as the serum dilution that produced 50% of maximal inhibition of colorimetric conversion of substrate xGAL by Hela cells infected with Ad-LacZ.

Statistical analysis

Data were analyzed using IBM SPSS Statistics version 18.0 Software (Chicago, Illinois) and expressed as mean ± standard errors of the mean (SEM). A minimum of four and usually five animals per group were analyzed individually in experiments, and the results shown represent one of at least two experiments, each of which showed the same trend and statistically significant differences (with $p<0.05$) in the observations emphasized in this study. We assessed significance ($p<0.05$) using the SPSS Univariate General Linear Model and one- or two-way analysis of variance (ANOVA) was followed by multiple t-tests.

Results

Oncostatin M stimulates iBALT formation and B cell accumulation and activation in the mouse lung

We and others have previously highlighted the ability of IL-6 overexpression to induce iBALT in the rodent lung (17, 27). IL-6 is well known to induce B cell expansion and stimulate antibody production (1,3), however, the role of the IL-6/gp130 family member OSM in B cell expansion and function is less clear. To test whether pulmonary delivery of transgenic OSM could induce iBALT formation, we endo-tracheally administered Ad-mOSM or empty vector (Ad-del70) to C57BL/6 mice and examined their lungs 7- and 14 days later. We found numerous lymphoid aggregates in lung parenchymal tissue of Ad-mOSM treated mice (Figure 1A, top panels), whereas control (Addel70-treated) lungs had scarce or no detectable inflammatory cell infiltrates (as previously observed (8, 25) and Figure 1B). We performed immunofluorescence on Ad-mOSM infected lungs and found that the lymphoid aggregates were mainly composed of large aggregates of $B220^+$ B cells, many of which expressed proliferating cell nuclear antigen (PCNA)(1A left lower panel, red and white stains) and bound peanut agglutinin (PNA) – a phenotype consistent with germinal center B cells (Figure 1A bottom panels). We found a few CD3+ T cells on the edge of the follicles (1A bottom middle panel, red stain) and $CD21^+CD35^+FDCM1^+$ follicular dendritic cells in the center of the B cell follicles (Figure 1A, bottom right panel, red stain). These data indicate that pulmonary OSM overexpression promotes iBALT formation.

To assess whether the Ad-mOSM-associated B cell activation and iBALT formation resulted in enhanced antibody (Ab) responses, we measured neutralizing Ab to adenovirus vector (see methods) in the serum, 24 days after primary infection and 7 days after a secondary infection (day 35) with Addel70. We found that Ad-mOSM-treated (but neither naïve nor Ad-del70-treated) animals had markedly increased titres of neutralizing Ab at day 24 (Figure 1C). We also found that the neutralizing titre increased a further 10-fold within 7 days after challenge with empty vector on day 28 (Figure 1C). In sharp contrast, challenge of naïve or Addl70 treated animals did not increase neutralizing Ab to detectable levels.

We next used flow cytometry to examine accumulation of $B220^+$ B cells and their activation status (CD69 and CD86 expression). Using the gating strategy outlined in Supplementary Figure 1, we found that mOSM expression elicited a 2-3-fold increase in the numbers of $B220^+$ B cells evident in the lung on day 7 and day 14 after infection (Figure 2A). As expected, numbers of $B220^+$ B cells in Ad-del70-infected animals were similar to uninfected controls. Ad-mOSM treatment increased the number of CD69-expressing ($CD69^{hi}$) and CD86-expressing ($CD86^{hi}$) B cells (Figure 2B). CD69- and CD86 expression on B cells, examined by mean fluorescence intensity (MFI), was significantly increased in Ad-mOSM-treated mice compared to Ad-del70-treated mice. In addition, marked eosinophilia was observed in lung tissue at days 7- and 14 days after Ad-mOSM administration (Figure 2C). These data demonstrated that OSM transgenic expression in lung induces B cell activation and accumulation of both B cells and eosinophils.

OSM stimulates accumulation and activation of pulmonary T cells and dendritic cells (DC)

To test whether transient transgenic OSM expression stimulated additional components of the adaptive immune system in the infected lungs, we examined the accumulation and activation DC, CD4+ and CD8+ T cells. We found that endo-tracheal administration of Ad-mOSM, but not control vector, induced a significant increase in the number of $CD4^+$ T cells in the lung at days 7 and 14 (Figure 3A). Although the numbers of CD8+ T cells were higher in Ad-mOSM-treated lungs, a statistically significant increase was not detected between the experimental groups (Figure 3B). However, at both 7- and 14 days post-Ad-mOSM-treatment, there was a statistically significant increase in CD69 surface expression and the numbers of activated (CD69-expressing), pulmonary $CD4^+$ and $CD8^+$ T cells, compared to the control Ad-del70 vector treated group (Figure 3A and 3B). Thus, in addition to B cell expansion, T cell accumulation and activation were increased as a result of pulmonary transgenic OSM expression.

Given that DCs are necessary for iBALT maintenance in response to viral infections (19), we next examined whether OSM transgenic expression could stimulate the accumulation and activation of DC, in parallel to iBALT formation. We found that Ad-mOSM-treatment elicited a significant increase in both the total number of $CD11c^{hi}$ MHC class II^{hi} DC and activated $CD86^+$ $CD11c^{hi}$ MHC class II^{hi} DC (Figure 3C), whereas the number of DC in control animals was similar to that in un-infected animals. Additionally, the frequency of CD86+ DC and the level of expression of CD86 on DC were significantly increased in lungs from Ad-mOSM-infected animals, compared to those from Ad-del70-infected or un-infected animals. These data demonstrate that mature, activated DCs accumulate in the lungs in response to transgenic OSM expression, a finding that could be potentially linked to participation of DCs in the formation of OSM-induced iBALT.

OSM-induced lung B- and T cell accumulation and activation are IL-6-independent

Since OSM is a potent inducer of IL-6 *in vitro* and in mouse lungs *in vivo* (25,28), OSM effects on B cells in this system could be due to IL-6 induction. To determine the role of IL-6 in lymphocyte accumulation, we endo-tracheally administered Ad-mOSM or control vectors to the lungs of WT and $IL\text{-}6^{-/-}$ mice (C57Bl/6 background) and evaluated DC, B- and T cell accumulation and activation. Surprisingly, IL-6-deficiency did not abrogate OSM-induced B cell accumulation and activation and, in fact, resulted in slightly increased numbers of total and CD69+ B cells compared to those in WT mice (Figure 4A). We also found that OSM-induced accumulation of $CD4^{+-}$ and $CD8^+$ T cells was normal in IL-6-/- mice (Figure 4B and C). Similarly, IL-6-deficiency neither affected OSM-induced increase in the number of $CD69^+$-activated $CD4^+$ T cells, nor the increased expression of CD69 on $CD4^+$ T cells (Figure 4B). However, there was a modest decrease in $CD69^+$ $CD8^+$ T cells in lungs of $IL\text{-}6^{-/-}$ mice, compared to lungs of WT mice (Figure 4C). CD69 expression on B cells and CD4 T cells, examined by MFI, was maintained at normal levels in $IL\text{-}6^{-/-}$ mice (panels on right for A-C). In addition, we found that IL-6-deficiency did not impair the accumulation of DC in Ad-mOSM-treated mice and that DC activation, as measured by CD86 expression, was even greater in the absence of IL-6 (Figure 4D). Together, these data indicate that OSM is capable of stimulating DC, B- and T cell lymphocyte accumulation and activation in the lungs in the absence of IL-6, highlighting the *in vivo* biological functions of

OSM executed independently of IL-6. The accumulation of eosinophils in the lung homogenates induced by Ad-mOSM was significantly reduced in IL-6-deficient mice compared to IL-$6^{-/-}$ at day 7, and although showed some reduction at day 14, the difference was not statistically significant (Figure 4E).

OSM stimulates iBALT formation independently of IL-6-signaling

We next enumerated iBALT structures in the lung tissue of WT and IL-$6^{-/-}$ mice treated with Ad-mOSM or control adenoviruses, two weeks after adenoviral vector delivery. We found that mice treated with Ad-mOSM, but not Ad-del70, developed lymphocytic cell aggregates in lung parenchymal tissue in both WT and IL-6-/- mice (Figure 5A). We observed a diffuse inflammatory cell infiltrate in the airspaces of Ad-mOSM-treated WT mice. At higher magnification (Fig 5B) inflammatory cells (examples of eosinophils indicated by arrowheads) were located in the alveolar interstitium. In contrast, accumulation of inflammatory cells in airspaces and the alveolar interstitium were less evident in Ad-mOSM-treated IL-6-/- mice. This is consistent with the analysis of lung tissue homogenates performed by flow cytometry (Fig 2C and 4E).

Immunofluorescence analysis demonstrated that Ad-mOSM, but not the Ad-del70 control, induced iBALT formation in both WT and IL-6-/- mice. iBALT was characterized by the presence of large B cell follicles containing PCNA+ proliferating B cells and $CD21^{+}CD35^{+}FDCM1^{+}$ follicular dendritic cells (Figure 5C). Total number of Ad-mOSM-induced ectopic lymphoid follicles was similar in WT and IL-$6^{-/-}$ mice. The total area covered by ectopic lymphoid follicles in the lungs of Ad-mOSM -treated IL-6-/- mice was actually larger (Figure 5D).

Maximal OSM-induced airway eosinophilia is IL-6-dependent

Given that Ad-mOSM-mediated iBALT formation and, B- and T cells were activated in a IL-6-independent fashion, we next assessed whether IL-6 played a role in OSM-induced eosinophil accumulation and chemokine expression. To test this possibility, we collected bronchoalveolar lavage (BAL) from Ad-mOSM- or Ad-del70-treated WT and IL-6-/- mice at day 7 after infection and enumerated inflammatory cells in cytospin preparations. As shown in Figure 6, numbers of macrophages, lymphocytes, neutrophils and eosinophils were significantly increased in Ad-mOSM-treated mice, compared to those in Ad-del70-treated and un-infected animals. However, the numbers of neutrophils eosinophils and lymphocytes, but not macrophages, were significantly decreased in the BAL of Ad-mOSM-treated IL-6-/- mice compared to those in WT mice. Decreases were also observed in the percentages of these cell types in the BAL fluid (Supplementary Figure 2). Thus IL-6-deficiency attenuates recruitment of innate inflammatory cells (eosinophils, neutrophils) to the airway alveolar spaces in response to OSM.

Impaired recruitment of inflammatory cells to the airways of IL-6-/- mice suggested that IL-6 may be controlling the local expression of inflammatory chemokines. To test this possibility, we next quantified the concentration of eotaxin-2, MCP-1 and KC as well as IL-6 in BAL fluid (Figure 6B). Consistent with changes observed in the total number of eosinophils, macrophages and neutrophils, we found that the levels of eotaxin-2, MCP-1 and

KC were elevated in BAL fluid of Ad-mOSM-treated WT mice, compared to Ad-mOSM-treated IL-6-/- mice. Although IL-6 was induced by Ad-mOSM in the BAL fluid of WT mice, it was not detectable in the BAL fluid of IL-6-/- mice. These data clearly suggest that IL-6 is selectively involved in OSM-mediated inflammatory cell trafficking in the airways, but not in OSM-induced iBALT formation.

OSM induces inflammatory cytokines and homeostatic chemokines

T helper cells and their cytokine products are critical for the generation of protective antibody responses. Since we previously observed that mOSM triggered the production of T_{h2} associated cytokines (25), we assessed whether T_{h2} cytokine expression induced by OSM was dependent on IL-6. Protein levels in BAL fluid from control or Ad-mOSM infected WT or IL-6-/- mice were examined 7 days after virus inoculation. As shown in Figure 7A, Ad-mOSM induced a significant increase in the T_{h2} cytokines IL-4, IL-5 and IL-10 as well as in the T_{h1} cytokines TNFα and IL-12. In contrast, OSM did not significantly increase IFNγ protein levels in BAL fluid (not shown). With the exception of IL-4, all the cytokines tested were produced in a IL-6-dependent manner.

Expression of homeostatic chemokines (HC), including CXCL13, CCL19 and CCL21 is generally associated with the formation and organization of iBALT structures (29). Moreover, the expression of CCL20 is associated with the formation of mucosal lymphoid tissues and the recruitment of DCs (30). Thus, we assessed the expression of HC in lungs of WT and IL-$6^{-/-}$ mice treated with the adenoviral vectors. We observed the B cell chemokine CXCL13 and DC chemokine CCL20 were elevated in lungs from Ad-mOSM-treated but not Addel70-treated WT mice (Figure 7B). CCL19 levels were either at or below the limit of detection of the ELISA (not shown). Finally, CCL21 protein levels remained unchanged or decreased in response to OSM (Figure 7B). Production of CXCL13 and CCL20, induced by Ad-mOSM inoculation, was markedly reduced in IL-6-/- mice, suggesting that other chemokines or cytokines may participate in the recruitment and organization of iBALT structures in the absence of IL-6.

Since OSM-induced IL-4 up-regulation was independent of IL-6 production (Fig 7), we assessed whether the IL-4/IL-13 signaling molecule STAT6 was required for Ad-mOSM-induced iBALT formation (Figure 8). Pictures of H&E stained lung tissue (top panels) show the presence of lymphocytic aggregates in STAT6-/- mice in response to Ad-mOSM administration. These ectopic lymphoid structures contained $B220^+$ cells, some of which were actively proliferating ($PCNA^+B220^+$), as well as FDC in the center of the B cell follicles (middle panels, lower panels a higher magnification of the same images). Morphometric analysis of ectopic lymphoid follicles shows a considerable increase in the number of lymphoid follicles in both wt and STAT6-/- mouse lungs in response to Ad-mOSM, but not Addel70 administration (Fig 8b). Collectively, this data (fig 5, 8) indicate that OSM-induced iBALT formation occurs independently of both IL-6 and STAT6.

Discussion

In this study, we showed that transient, transgenic expression of OSM in mouse lungs using adenovirus vector elicited marked accumulation of activated B cells at day 7- and 14 post-

infection and promoted iBALT formation, particularly in lung parenchyma. The Ad-mOSM vector induced increases in the number and activation of DC, $CD4^+$ and $CD8^+$ T cells, although to a lesser extent than those changes in B cells. These changes were associated with elevated levels of HC that support iBALT formation and likely influenced production of neutralizing Ab to adenovirus. Importantly, none of these effects were seen in mice receiving control adenovirus. The results suggested that, in the context of respiratory infection, elevated levels of mOSM induce a profound B cell response and iBALT formation in C57Bl/6 mice. We have also observed similar lymphocyte aggregate formation in BALB/c mice upon endotracheal administration of Ad-mOSM (data not shown), suggesting these observations are not peculiar to the C57Bl/6 strain. The elevation of neutralizing anti-adenovirus antibody titre could be associated with the iBALT formation, and Ad-mOSM appears to act with an adjuvant-like effect in this scenario, boosting the response to a subsequent lung challenge (of empty vector). The neutralizing antibodies are likely directed against the penton base and/or fibre protein that are important in infection of cells by the virus. Whether antibodies to other antigens or potential pathogens can be produced using this system awaits further analysis.

The function of OSM in human lung inflammation and disease is not yet clear and our present studies suggest that OSM might be involved in iBALT formation in human disease. The bronchus-associated lymphoid tissue (BALT) was first identified many years ago (31) and is considered part of the common mucosal immune system. Inducible BALT forms in response to infection or inflammation (18) and a number of human pathologies are associated with iBALT formation, including lung complications of rheumatoid arthritis (RA) (21). Interestingly, elevated OSM has been detected in RA synovial tissues and fluids (32) where there is formation of ectopic lymphoid tissues. However it is not known whether RA patients with lung complications show elevated OSM in lung tissue. Lungs from patients with idiopathic pulmonary fibrosis (IPF) display increased iBALT formation (33), coinciding with elevated OSM levels in BAL fluid (11). Another interesting observation is the formation of iBALT in lung tissue from asthmatic patients (34) and detection of OSM in BAL of patients suffering severe asthma (9). iBALT has been detected in chronic smokers (34) raising the question of whether such effects might be explained by production of OSM by activated macrophages. Although OSM has been detected in neutrophils and eosinophils, activated macrophages and T cells are the major cell sources of high amounts of OSM (as seen in RA synovial fluid). Altogether, these cells could add to the load of active OSM in inflammatory lung tissue. Therefore, our observations support the rationale for further study of the contribution of OSM in lung disease.

Previous work shows that sustained transgenic over-expression of IL-6 together with its soluble receptor (sIL-6R) in the lung induces iBALT formation primarily in subepithelial areas(17). In contrast, following Ad-mOSM administration, we primarily observed iBALT in the lung parenchyma. In Ad vector systems, encoded cytokines are typically expressed for a brief period of 4-12 days (27) and although expression is relatively high, these transient systems allow examination of potential effects of cytokines with less concern than long term transgenic systems. The current lack of effective systems for quantitatively measuring mouse OSM protein precludes our ability to determine OSM levels in our system or other mouse models of inflammation or disease and this is a limitation in our study. In previous

work using Advector but expressing GMCSF in mouse lung, GMCSF levels in BAL ranged from pg/ml to peak levels at day 4 (approx 8 ng/ml) and then declined by day 12 (39). Analysis of OSM in human BAL samples of IPF patients were in the 100 pg/ml range (11) while OSM levels in induced sputum of severe asthmatic patients included values at over 1 ng/ml (9). Such studies on clinical samples may or may not capture peaks of OSM detectable in human tissues in context of disease progression. Thus, we believe our study supports further investigation into the potential role of OSM over-expression in lung disease. In addition, our observations in the mouse are not restricted to Ad vector - induced OSM effects, since Mossifarian et al (11) have found effects in eosinophil accumulation or ECM accumulation after 10 days of administration of recombinant OSM protein (2 micrograms daily) that resemble the observations we have made in our model of pulmonary delivery of Ad-OSM (8)(25). Loss of function studies in future work would further clarify the role of OSM in models of lung disease.

One difference in our studies and those using constitutive long- term transgenes may be due to the timing of expression. Previous work shows that overexpression of human IL-6 (with sIL-6R) by Ad vectors in rat lungs leads to a transient lymphocytic alveolitis (35), whereas the overexpression of rat IL-6 by Ad vector leads to iBALT formation, primarily located in subepithelial locations (27). In contrast to this previous work, the iBALT in our Ad-mOSM system here was remarkably pronounced in the lung parenchyma, supporting the concept of separate mechanisms of OSM from those exerted by IL-6 overexpression.

Despite the ability of IL-6 to generate iBALT (17), we found that iBALT formation and B cell accumulation occurred in the lungs of Ad-OSM-treated IL-$6^{-/-}$ mice, consistent with the IL-6-independent effect of OSM on iBALT formation. In contrast, pulmonary inflammation, including cell infiltration into broncholaveolar spaces as well as the elevated expression of inflammatory chemokines (eotaxin-2, KC and MCP-1) and cytokines (IL-5, IL-10, TNFα and IL-12), were all highly dependent on IL-6. The accumulation of eosinophils in the lung tissue as measured by flow cytometry of lung homogenates in Fig 2C,4E, and in alveolar interstitium in sample histology sections (fig 5B), suggests that eosinophilic infiltrates occurred in the interstitial lung compartments as well as in the alveolar spaces (as measured in BAL in Fig 6) due to Ad-mOSM in wt mice. Detection of markedly lower eosinophils in the lung homogenates at day 7 (Fig 4E), histological sections (Fig 5B) and in BAL (Fig 6) of IL-6-/- mice after Ad-OSM administration suggests that IL-6 participates in recruitment of eosinophils to both the alveolar lumen and lung tissue compartments. In contrast, IL-6 deficiency had no detectable affect on the formation/organization of iBALT in the lung tissue. Thus the IL-6-/- deficiency was reflected in reduced inflammation in lungs due to Ad-mOSM in this system, and these results collectively demonstrate that OSM acts through IL-6-dependent and -independent pathways to mediate its effects in the mouse lung.

Our previous studies show that Ad-mOSM induces Th2 cytokine production and eosinophil accumulation in the lungs (8) and that these effects are dependent on the signaling molecule STAT6 (25). Our results are consistent with previous observations (25), including up-regulation of IL-4, IL-5, IL-10 but not IFNγ. Surprisingly, both IL-12 and TNF were produced in the lung of Ad-mOSM-treated mice, suggesting that OSM overexpression does not exclusively induce Th2 skewing in the C57Bl/6 mouse lung. These results further show

that IL-6 is required for optimal production of inflammatory chemokines and eosinophil accumulation in C57Bl/6 mice. IL-6 deficiency did not affect IL-4 concentration in BAL (Fig 6), suggesting that there could be activation of the STAT-6 signaling pathway. However, we observed iBALT formation in STAT6-/- mice upon Ad-mOSM administration (Fig 8). This indicated that STAT6 signaling, typically activated by the classic T_{h2} cytokines IL-4 or IL-13, is not required for iBALT formation elicited by Ad-mOSM. Collectively, the results suggest a unique function for OSM in inducing B cell activation and parenchymal iBALT formation.

HC CXCL13, CXCL19, CCL21 and CCL20 are expressed in iBALT structures and together regulate iBALT formation, organization and function (29). In addition, mOSM upregulates CCL21 expression, a potent dendritic cell chemoattractant (36, 37) in the skin. After examining BAL levels of HC at day 7 after infection (Figure 7), we observed increases in CXCL13 and CCL20 protein concentration, a reduction in CCL21 protein levels and low/undetectable levels of CCL19. Reduced CCL21 expression has been previously observed after pulmonary infection with influenza (20). This suggests that OSM over-expression is preferentially inducing production of the B cell chemokines CXCL13 and CCL20. Unexpectedly, none of these chemokines was elevated in IL-$6^{-/-}$ mice by Ad-mOSM (Figure 7), thus suggesting the participation of non-classical molecules on iBALT formation. Alternatively, we might have missed earlier peaks of HC expression that could have been sufficient for supporting the initial waves of iBALT formation in the IL-$6^{-/-}$ animals. The precise mechanism by which mOSM supports iBALT formation in either WT or IL-$6^{-/-}$ mice requires further study and might involve $CD4^+$ follicular helper T cells (T_{FH}), which are known to facilitate B cell follicle expansion, through expression of IL-21 (38). Overall, our results suggest that mOSM induces iBALT formation independently of IL-6, occurs in the presence of low levels of classic HC (CCL19, CCL20, CCL21, CXCL13) and in the absence of STAT6 signaling. Collectively, these findings support a unique role for OSM in lung mucosal immunity and inflammation. OSM-mediated formation of iBALT in our system suggests that elevated production of OSM in human diseases such as IPF, RA or asthma could explain the formation of iBALT and ectopic lymphoid structures, which are likely linked to the perpetuation of chronic inflammation and the consequent pathological tissue damage.

Supplementary Material

Refer to Web version on PubMed Central for supplementary material.

Acknowledgments

The authors gratefully acknowledge the expert technical support of Jane Ann Smith and Rebecca Rodrigues, and assistance from Sean Lauber, Jessica Guerette and David Schnittker. We also thank Dr. Mark McDermott for critical reading of the manuscript.

References

1. Silver JS, Hunter CA. gp130 at the nexus of inflammation, autoimmunity, and cancer. J Leukoc Biol. 2010; 88:1145–1156. [PubMed: 20610800]

2. Heinrich PC, Behrmann I, Haan S, Hermanns HM, Müller-Newen G, Schaper F. Principles of interleukin (IL)-6-type cytokine signalling and its regulation. The Biochemical journal. 2003; 374:1–20. [PubMed: 12773095]

3. Tanaka M, Miyajima A. Oncostatin M, a multifunctional cytokine. Reviews of physiology, biochemistry and pharmacology. 2003; 149:39–52.

4. Faffe DS, Flynt L, Mellema M, Moore PE, Silverman ES, Subramaniam V, Jones MR, Mizgerd JP, Whitehead T, Imrich A, Panettieri RA, Shore SA. Oncostatin M causes eotaxin-1 release from airway smooth muscle: synergy with IL-4 and IL-13. The Journal of allergy and clinical immunology. 2005; 115:514–520. [PubMed: 15753898]

5. Fritz DK, Kerr C, Tong L, Smyth D, Richards CD. Oncostatin-M up-regulates VCAM-1 and synergizes with IL-4 in eotaxin expression: involvement of STAT6. Journal of immunology. 2006; 176:4352–4360.

6. Hintzen C, Haan C, Tuckermann JP, Heinrich PC, Hermanns HM. Oncostatin M-induced and constitutive activation of the JAK2/STAT5/CIS pathway suppresses CCL1, but not CCL7 and CCL8, chemokine expression. The Journal of Immunology. 2008; 181:7341–7349. [PubMed: 18981157]

7. Lafontant PJ, Burns AR, Donnachie E, Haudek SB, Smith CW, Entman ML. Oncostatin M differentially regulates CXC chemokines in mouse cardiac fibroblasts. American journal of physiology Cell physiology. 2006; 291:C18–26. [PubMed: 16452159]

8. Langdon C, Kerr C, Tong L, Richards CD. Oncostatin M regulates eotaxin expression in fibroblasts and eosinophilic inflammation in C57BL/6 mice. Journal of Immunology. 2003; 170:548–555.

9. Simpson JL, Baines KJ, Boyle MJ, Scott RJ, Gibson PG. Oncostatin M (OSM) is increased in asthma with incompletely reversible airflow obstruction. Experimental lung research. 2009; 35:781–794. [PubMed: 19916861]

10. Kang HJ, Kang JS, Lee SH, Hwang SJ, Chae SW, Woo JS, Lee HM. Upregulation of oncostatin m in allergic rhinitis. The Laryngoscope. 2005; 115:2213–2216. [PubMed: 16369169]

11. Mozaffarian A, Brewer AW, Trueblood ES, Luzina IG, Todd NW, Atamas SP, Arnett HA. Mechanisms of oncostatin M-induced pulmonary inflammation and fibrosis. The Journal of Immunology. 2008; 181:7243–7253. [PubMed: 18981146]

12. Nightingale J, Patel S, Suzuki N, Buxton R, Takagi Ki, Suzuki J, Sumi Y, Imaizumi A, Mason RM, Zhang Z. Oncostatin M, a cytokine released by activated mononuclear cells, induces epithelial cell-myofibroblast transdifferentiation via Jak/Stat pathway activation. Journal of the American Society of Nephrology : JASN. 2004; 15:21–32. [PubMed: 14694154]

13. Goren I, Kämpfer H, Müller E, Schiefelbein D, Pfeilschifter J, Frank S. Oncostatin M expression is functionally connected to neutrophils in the early inflammatory phase of skin repair: implications for normal and diabetes-impaired wounds. The Journal of investigative dermatology. 2006; 126:628–637. [PubMed: 16410783]

14. Jung ID, Noh KT, Lee CM, Chun SH, Jeong SK, Park JW, Park WS, Kim HW, Yun CH, Shin YK, Park YM. Oncostatin M induces dendritic cell maturation and Th1 polarization. Biochem Biophys Res Commun. 2010; 394:272–278. [PubMed: 20206608]

15. Louis I, Dulude G, Corneau S, Brochu S, Boileau C, Meunier C, Côté C, Labrecque N, Perreault C. Changes in the lymph node microenvironment induced by oncostatin M. Blood. 2003; 102:1397–1404. [PubMed: 12702501]

16. Clegg CH, Haugen HS, Rulffes JT, Friend SL, Farr AG. Oncostatin M transforms lymphoid tissue function in transgenic mice by stimulating lymph node T-cell development and thymus autoantibody production. Experimental hematology. 1999; 27:712–725. [PubMed: 10210329]

17. Goya S, Matsuoka H, Mori M, Morishita H, Kida H, Kobashi Y, Kato T, Taguchi Y, Osaki T, Tachibana I, Nishimoto N, Yoshizaki K, Kawase I, Hayashi S. Sustained interleukin-6 signalling leads to the development of lymphoid organ-like structures in the lung. The Journal of pathology. 2003; 200:82–87. [PubMed: 12692845]

18. Foo SY, Phipps S. Regulation of inducible BALT formation and contribution to immunity and pathology. Mucosal immunology. 2010; 3:537–544. [PubMed: 20811344]

19. GeurtsvanKessel CH, Willart MAM, Bergen IM, van Rijt LS, Muskens F, Elewaut D, Osterhaus ADME, Hendriks R, Rimmelzwaan GF, Lambrecht BN. Dendritic cells are crucial for

maintenance of tertiary lymphoid structures in the lung of influenza virus-infected mice. J Exp Med. 2009; 206:2339–2349. [PubMed: 19808255]

20. Moyron-Quiroz JE, Rangel-Moreno J, Kusser K, Hartson L, Sprague F, Goodrich S, Woodland DL, Lund FE, Randall TD. Role of inducible bronchus associated lymphoid tissue (iBALT) in respiratory immunity. Nat Med. 2004; 10:927–934. [PubMed: 15311275]
21. Rangel-Moreno J, Hartson L, Navarro C, Gaxiola M, Selman M, Randall TD. Inducible bronchus-associated lymphoid tissue (iBALT) in patients with pulmonary complications of rheumatoid arthritis. The Journal of clinical investigation. 2006; 116:3183–3194. [PubMed: 17143328]
22. Kahnert A, Höpken UE, Stein M, Bandermann S, Lipp M, Kaufmann SHE. Mycobacterium tuberculosis triggers formation of lymphoid structure in murine lungs. The Journal of infectious diseases. 2007; 195:46–54. [PubMed: 17152008]
23. Bánfi A, Tiszlavicz L, Székely E, Peták F, Tóth-Szüki V, Baráti L, Bari F, Novák Z. Development of bronchus-associated lymphoid tissue hyperplasia following lipopolysaccharide-induced lung inflammation in rats. Experimental lung research. 2009; 35:186–197. [PubMed: 19337902]
24. Fleige H, Haas JD, Stahl FR, Willenzon S, Prinz I, Förster R. Induction of BALT in the absence of IL-17. Nature Immunology. 2012; 13 1-author reply 2.
25. Fritz DK, Kerr C, Fattouh R, Llop-Guevara A, Khan WI, Jordana M, Richards CD. A mouse model of airway disease: oncostatin M-induced pulmonary eosinophilia, goblet cell hyperplasia, and airway hyperresponsiveness are STAT6 dependent, and interstitial pulmonary fibrosis is STAT6 independent. The Journal of Immunology. 2011; 186:1107–1118. [PubMed: 21160052]
26. Rangel-Moreno J, Carragher DM, de la Luz Garcia-Hernandez M, Hwang JY, Kusser K, Hartson L, Kolls JK, Khader SA, Randall TD. The development of inducible bronchus-associated lymphoid tissue depends on IL-17. Nature Publishing Group. 2011; 12:639–646.
27. Xing Z, Braciak T, Jordana M, Croitoru K, Graham FL, Gauldie J. Adenovirus-mediated cytokine gene transfer at tissue sites. Overexpression of IL-6 induces lymphocytic hyperplasia in the lung. Journal of Immunology. 1994; 153:4059–4069.
28. Bilsborough J, Mudri S, Chadwick E, Harder B, Dillon SR. IL-31 receptor (IL-31RA) knockout mice exhibit elevated responsiveness to oncostatin M. The Journal of Immunology. 2010; 185:6023–6030. [PubMed: 20956341]
29. Rangel-Moreno J, Moyron-Quiroz JE, Hartson L, Kusser K, Randall TD. Pulmonary expression of CXC chemokine ligand 13, CC chemokine ligand 19, and CC chemokine ligand 21 is essential for local immunity to influenza. Proc Natl Acad Sci U S A. 2007; 104:10577–10582. [PubMed: 17563386]
30. Schutyser E, Struyf S, Van Damme J. The CC chemokine CCL20 and its receptor CCR6. Cytokine & growth factor reviews. 2003; 14:409–426. [PubMed: 12948524]
31. McDermott MR, Befus AD, Bienenstock J. The structural basis for immunity in the respiratory tract. International review of experimental pathology. 1982; 23:47–112. [PubMed: 7045014]
32. Cawston TE, Curry VA, Summers CA, Clark IM, Riley GP, Life PF, Spaull JR, Goldring MB, Koshy PJ, Rowan AD, Shingleton WD. The role of oncostatin M in animal and human connective tissue collagen turnover and its localization within the rheumatoid joint. Arthritis Rheum. 1998; 41:1760–1771. [PubMed: 9778217]
33. Marchal-Sommé J, Uzunhan Y, Marchand-Adam S, Valeyre D, Soumelis V, Crestani B, Soler P. Cutting edge: nonproliferating mature immune cells form a novel type of organized lymphoid structure in idiopathic pulmonary fibrosis. Journal of immunology. 2006; 176:5735–5739.
34. Elliot JG. Aggregations of Lymphoid Cells in the Airways of Nonsmokers, Smokers, and Subjects with Asthma. American journal of respiratory and critical care medicine. 2004; 169:712–718. [PubMed: 14711796]
35. Yoshida M, Sakuma J, Hayashi S, Abe K, Saito I, Harada S, Sakatani M, Yamamoto S, Matsumoto N, Kaneda Y. A histologically distinctive interstitial pneumonia induced by overexpression of the interleukin 6, transforming growth factor beta 1, or platelet-derived growth factor B gene. Proc Natl Acad Sci U S A. 1995; 92:9570–9574. [PubMed: 7568174]
36. Sugaya M, Fang L, Cardones AR, Kakinuma T, Jaber SH, Blauvelt A, Hwang ST. Oncostatin M enhances CCL21 expression by microvascular endothelial cells and increases the efficiency of dendritic cell trafficking to lymph nodes. Journal of immunology. 2006; 177:7665–7672.

37. Le Borgne M, Etchart N, Goubier A, Lira SA, Sirard JC, van Rooijen N, Caux C, Aït-Yahia S, Vicari A, Kaiserlian D, Dubois B. Dendritic cells rapidly recruited into epithelial tissues via CCR6/CCL20 are responsible for CD8+ T cell crosspriming in vivo. Immunity. 2006; 24:191–201. [PubMed: 16473831]

38. Nurieva RI, Chung Y, Hwang D, Yang XO, Kang HS, Ma L, Wang YH, Watowich SS, Jetten AM, Tian Q, Dong C. Generation of T Follicular Helper Cells Is Mediated by Interleukin-21 but Independent of T Helper 1, 2, or 17 Cell Lineages. Immunity. 2008; 29:138–149. [PubMed: 18599325]

39. Wang J, Snider DP, Hewlett BR, Lukacs NW, Gauldie J, Liang H, Xing Z. Transgenic expression of granulocyte colony-stimulating factor induces the differentiation and activation of a novel dendritic cell population in the lung. Blood. 2000; 95:2337–2345. [PubMed: 10733504]

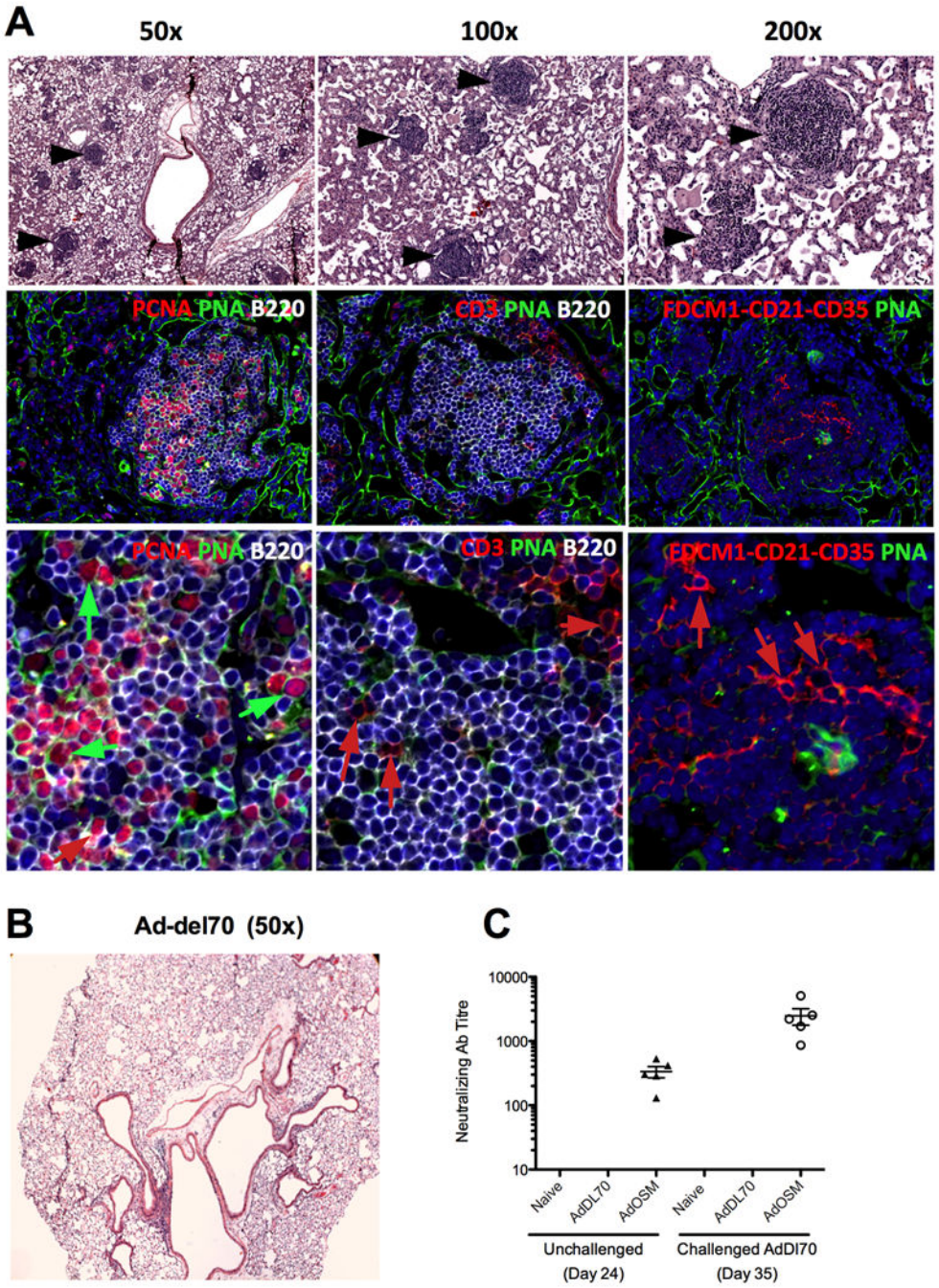

Figure 1. Assessment of iBALT formation in mouse lung upon administration of Ad-mOSM

(A) C57Bl/6 mice were endo-tracheally inoculated with 5×10^7 PFUs of Ad-del70 control adenovirus or Ad-mOSM adenovirus and sacrificed 14 days later. Whole lung tissue was fixed in 10% formalin and stained with hematoxylin and eosin. (A) Lymphocytic aggregates were readily apparent (black arrows in top row of panels) at lower- and high magnification (50×-200×). Representative images from Ad-mOSM- (A) or Ad-del70 treated mice (B) are shown. In second and third rows (higher magnification), tissues were stained with antibodies against B220 for detecting B cells (B220, white surface stain), proliferating cells

(proliferating cell nuclear antigen: PCNA, red nuclear stain, left panels) and T cells (CD3, red surface stain, middle panels, red arrows). Large, proliferating large B blasts (PCNA +PNA+B220+, green arrows in left panels), located inside germinal centres stain positive for peanut agglutinin (PNA, green). Follicular dendritic cells were detected with a combination of antibodies against FDC antigen, CD21 and CD35, (red surface stain, right panels, red arrows). DAPI was used to stain nuclei (shown in blue). Images are representative of all aggregates. (C) Neutralizing antibody (Ab) titre induced by Ad-mOSM treatments was measured at day 24 post-inoculation in serum from naïve, Ad-del70 and Ad-mOSM treated animals (left). Titres were also measured at day 35 in the serum of the same animals which were challenged (endotracheal administration at day 28) with Addel70 (right). Titres were not detectable at level of sensitivity (<40 dilution) in naïve or Addel70 treatments either with or without Addl70 challenge. Representative results from one experiment of two that generated the same trend are shown (n=5/group).

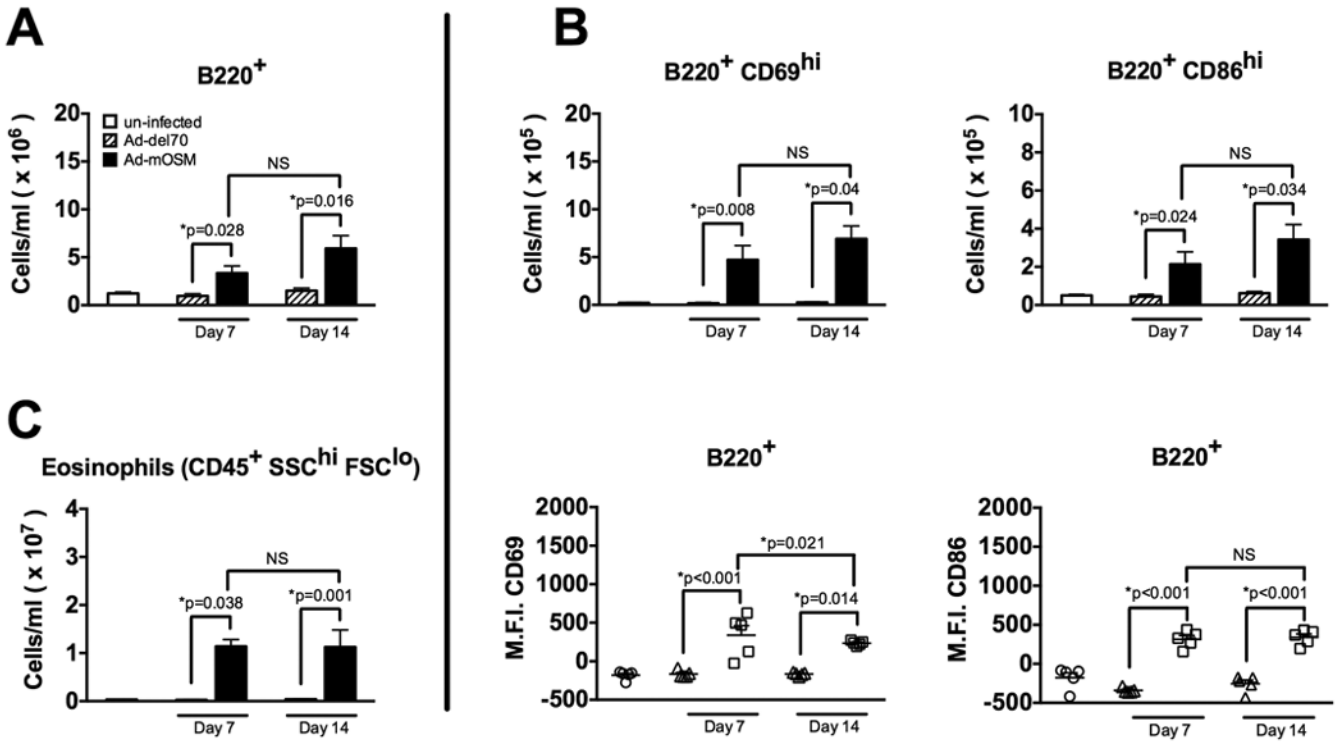

Figure 2. FACS analysis of pulmonary B cells in Ad-mOSM treated mouse lungs

A. $B220^+$ B cells were enumerated by flow cytometry on days 7 and 14 after inoculation with Ad-mOSM, Ad-del70 or PBS. B. Expression of the activation markers CD69 and CD86 were examined on lung $B220^+$ B cells from un-infected, day 7 and day 14 Ad-del70- or Ad-OSM-infected (top panels in B). Mean fluorescence intensity (M.F.I.) for CD69 and CD86 expression on $B220^+$ cells is shown (bottom panels in B). C. Eosinophils were enumerated by flow cytometry in the same lung tissues. $CD45^+$ live cells in the high side scatter (SSC) and low forward scatter (FSC) gate were identified as eosinophils, whereas $CD45^+$ live cells with a low SSC and low FSC profile were identified as lymphocytes. Total numbers for $B220^+$ B cells, CD69- and CD86 high-expressing (hi) cells, $B220^+$ CD86-hi cells and eosinophils ($CD45^+$ SSC-hi FSC-lo) are shown. Results are presented as the means ± SEMs of at least five mice per group. Data shown is representative of at least two separate experiments.

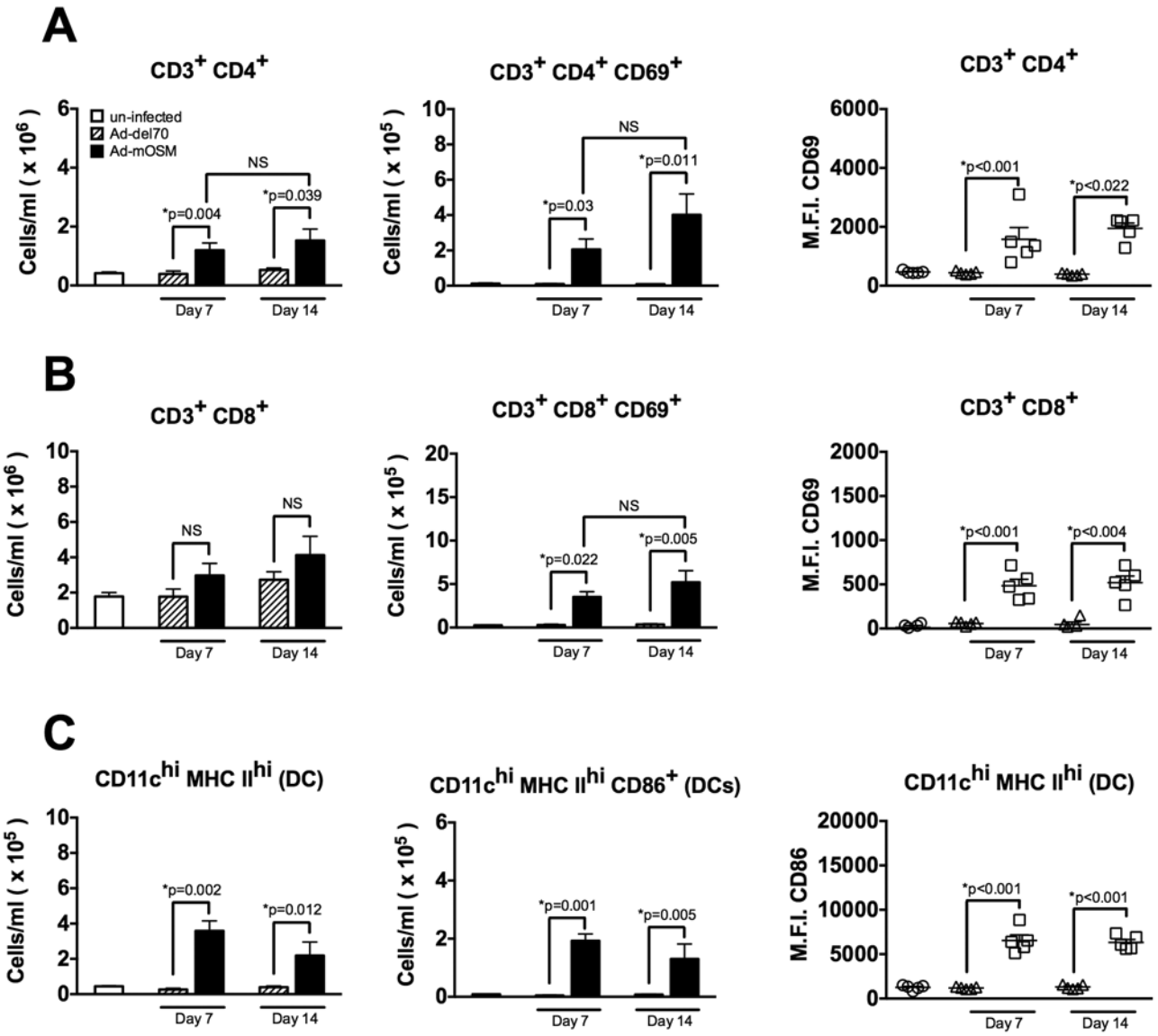

Figure 3. FACS analysis of pulmonary T cells and dendritic cells in Ad-mOSM treated mice

(A) C57Bl/6 mice were inoculated with Ad-del70 or Ad-mOSM adenovirus or no virus (un-infected). Total numbers of CD3-, CD4- and CD8 T cells, and their respective CD69 expression, were examined by flow cytometry at 7- or 14 days after adenovirus inoculation. Total numbers of lung infiltrating (A) $CD4^+$ T cells, $CD4^+$ $CD69^+$ T cells, (B) $CD8^+$ T cells, $CD8^+$ $CD69^+$ T cells. CD69 mean fluorescence intensity (M.F.I.) for $CD4^+$ and $CD8^+$ T cells is shown in right panels for A and B. (C) Total numbers of pulmonary CD11c-hi MHC class II-hi (MHC II^{hi}) dendritic cells (left panel), $CD86^+$ dendritic cells (middle panel) and CD86 M.F.I. levels on dendritic cells (right panel) were examined by flow cytometry as described in (A). Results are expressed as the means ± SEMs of at least five mice per group. Representative data from at least two separate experiments, with similar results, is shown.

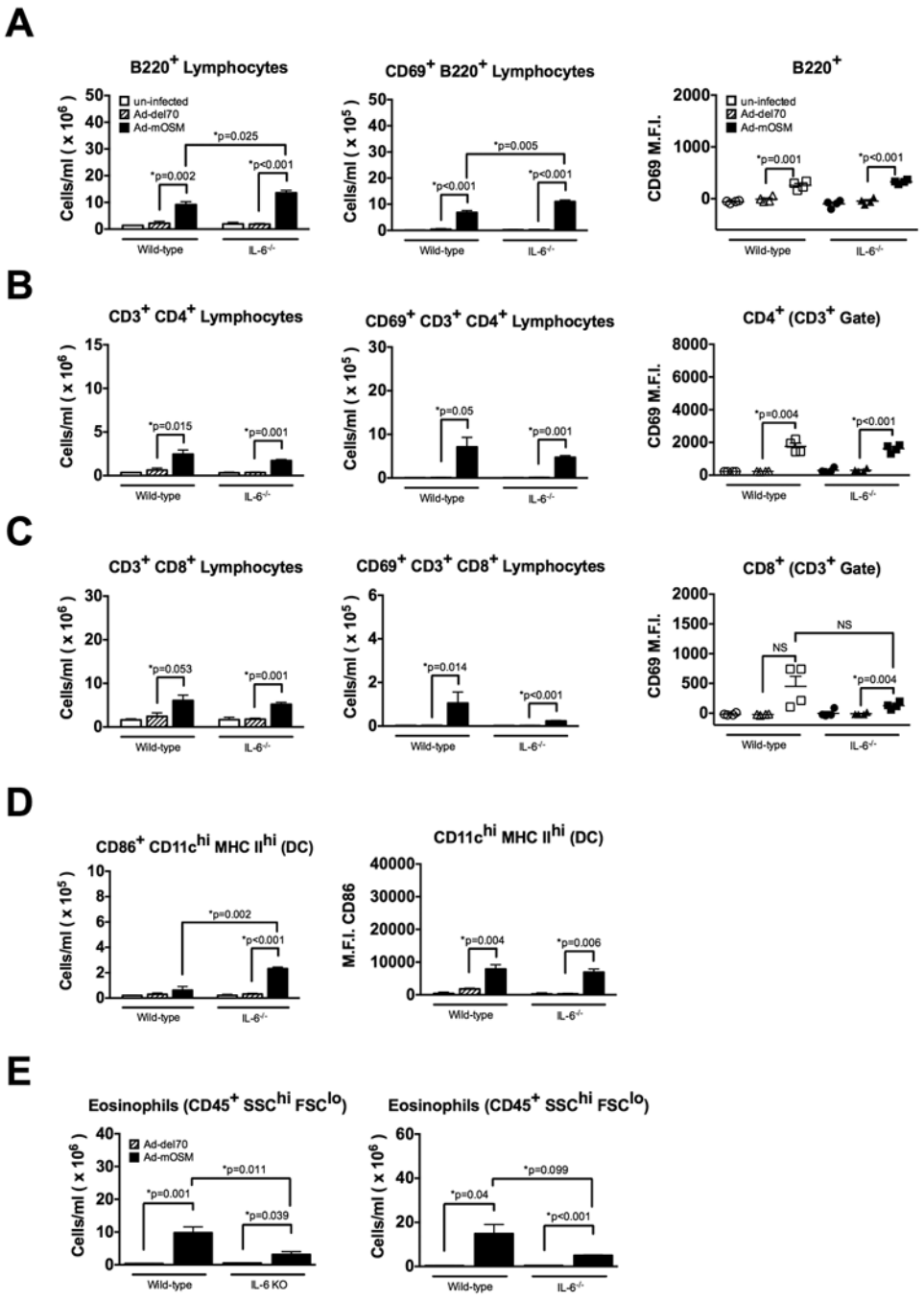

Figure 4. FACS analysis of lung B cells, T cells, DC and eosinophils in wild-type and IL-6$^{-/-}$ mice upon Ad-mOSM treatment

C57Bl/6 wild-type and IL-6-gene-deficient knock-out (IL-6$^{-/-}$) mice were inoculated with Ad-del70, Ad-mOSM adenovirus or no virus (un-infected). Total numbers of B220+ B cells, CD4^{+}- and CD8^{+} T cells, as well as the expression of CD69 on them were examined, at day 14 following adenovirus inoculation as described in Figures 2 and 3. Total lung tissue numbers of B220^{+}, CD69^{+} B220^{+} B cells (A), CD4^{+}, CD4^{+} CD69^{+} T cells (B), CD8^{+}, CD8^{+} CD69^{+} T cells (C) dendritic cells (D) and eosinophils (E) at day 7 (left panel) and Day 14 (right panel) are shown. CD69 mean fluorescence intensity (M.F.I.) is shown in right

panels for A-C. Results are presented as the means ± SEMs of at least five mice per group. Representative data of two separate experiments, with similar results, is shown.

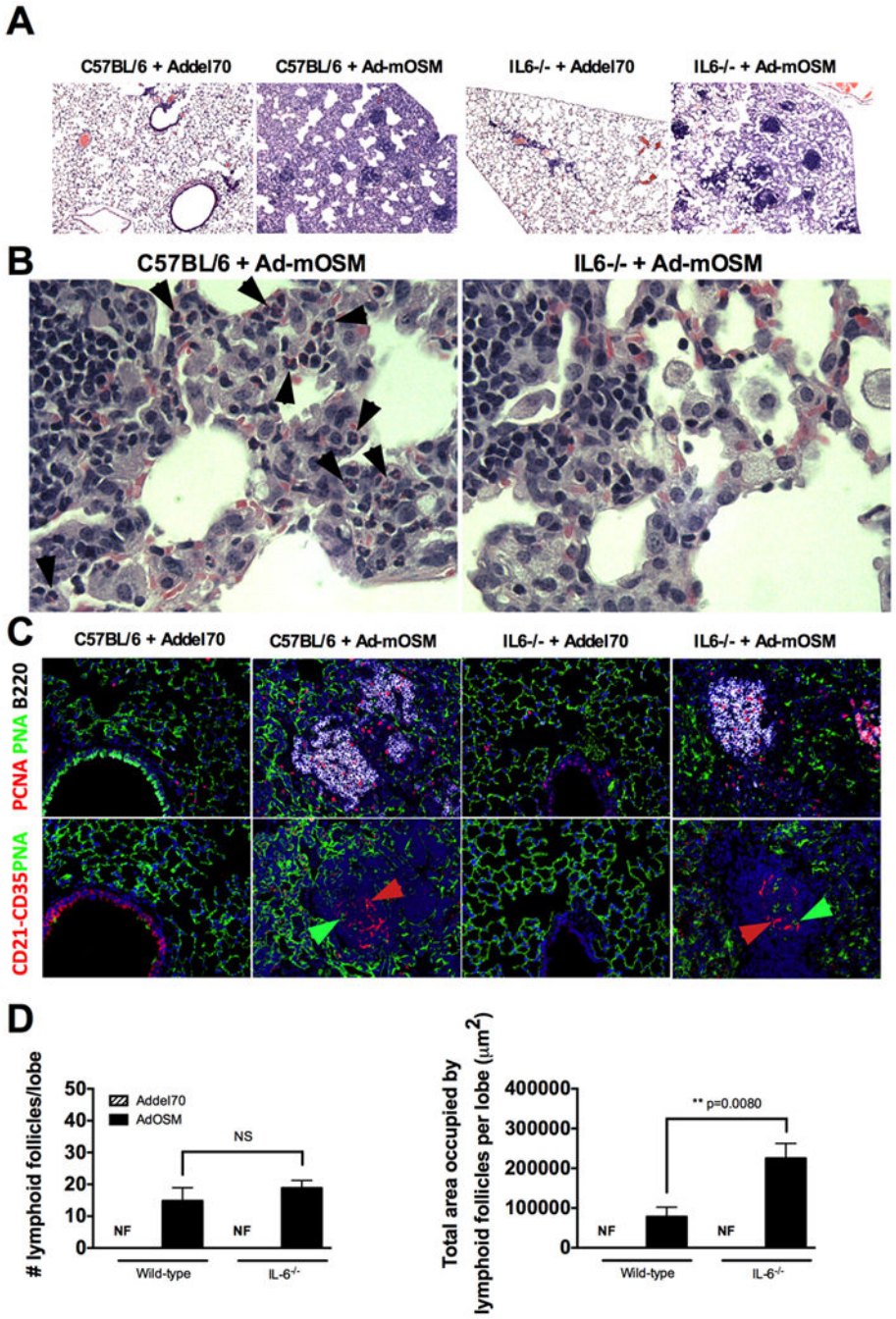

Figure 5. Assessment of iBALT formation in wild-type and IL-6$^{-/-}$ mice upon Ad-mOSM treatment

C57Bl/6 wild-type and IL-6$^{-/-}$ mice were inoculated with Ad-del70 or Ad-mOSM, as described in Figure 1. Formalin-fixed, paraffin embedded lung sections, stained with H&E, were examined for the presence of iBALT. Lung tissue sections display distinctive lymphocytic aggregates within lung parenchyma. (A, low power) and accumulation of inflammatory cells (B, higher power, arrows point to eosinophils). (C), Complexity of iBALT structures was evaluated by staining with antibodies for B220 (B cells, white surface stain), FDCM1, CD21 and CD35 (follicular dendritic cells, red surface stain, red arrows)

and proliferating cell nuclear antigen (PCNA, red nuclear stain). Fluorescent, peanut agglutinin lectin was used to detect large proliferating B blasts ($PCNA^{+}PNA^{+}B220^{+}$) inside germinal centers (PNA, green surface stain, green arrows). (D) Number of lymphoid follicles per lung lobe (left) and total area occupied by lymphoid follicles per lung lobe (right), in C57BL/6 and IL-$6^{-/-}$ mice, inoculated with Ad-del70 or Ad-mOSM is shown.

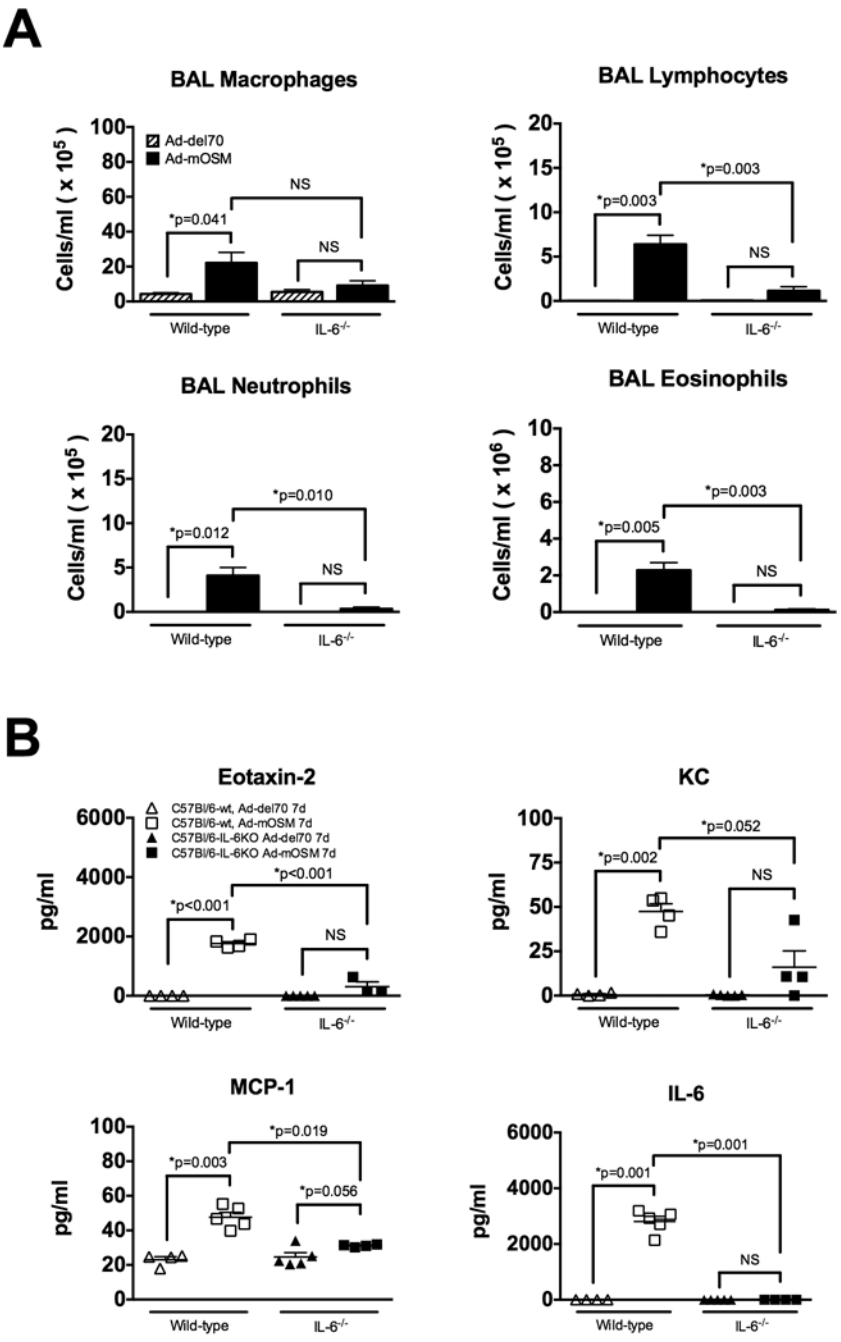

Figure 6. Ad-mOSM-induced airway leukocyte accumulation and chemokine expression in wild-type and Il6$^{-/-}$ mice

C57Bl/6- and IL-6$^{-/-}$ mice were inoculated with Ad-del70, Ad-mOSM adenovirus or PBS (un-infected). Mouse BAL fluid was collected 7 days after infection. Cytospins preparations were stained with Hema-3. (A) Numbers of macrophages, lymphocytes, neutrophils and eosinophils in the BAL were determined as described in materials and methods. (B) Concentration of eotaxin-2, KC, MCP-1, and IL-6 in BAL fluid was measured by ELISA. Results represent the means ± SEMs of at least four mice per group. Data shown is representative of at least two separate experiments.

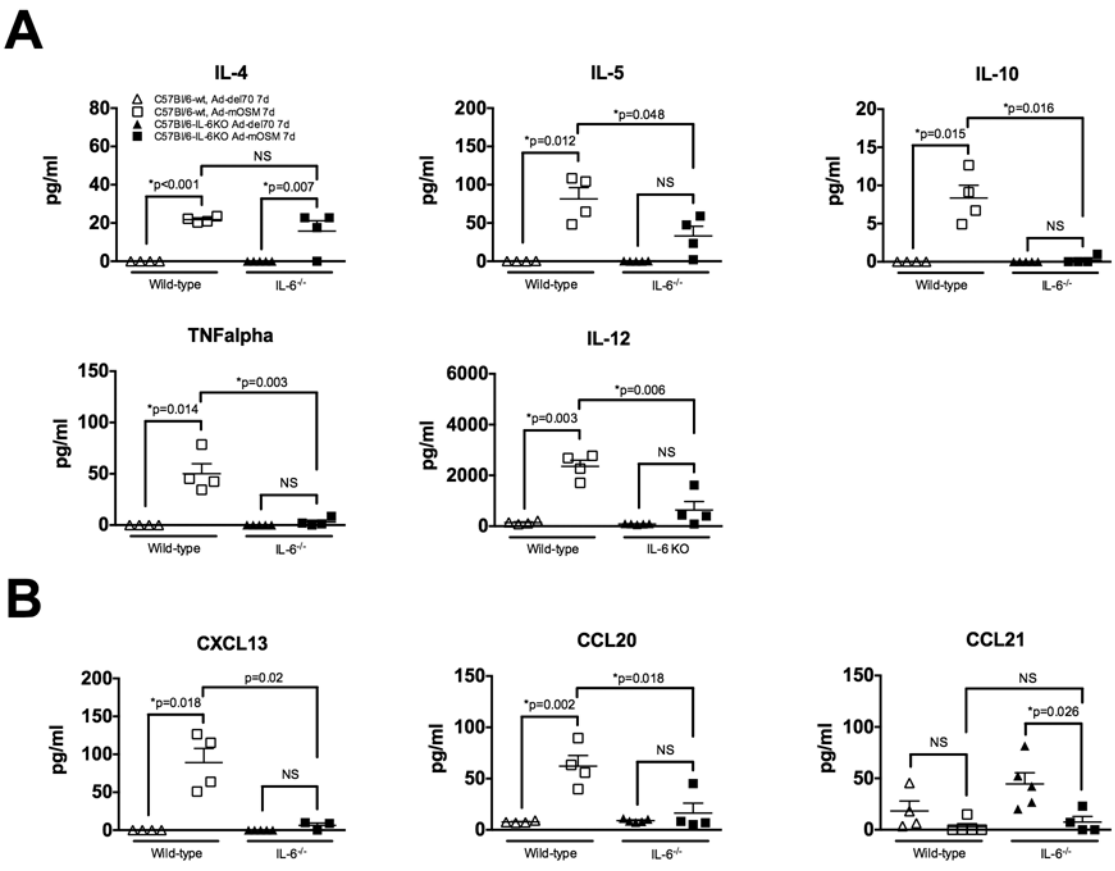

Figure 7. Levels of Th1, Th2 and iBALT-associated chemokines in wild-type and IL-6$^{-/-}$ mice following endo-tracheal administration with Ad-mOSM

C57Bl/6- and IL-6$^{-/-}$ mice were inoculated with Ad-del70, Ad-mOSM adenovirus or PBS (un-infected). BAL fluid was collected 7 days after infection to quantify protein levels of T_{h1}-, T_{h2} cytokines and iBALT-associated chemokines. (A) Protein concentration of the typical T_{h2} cytokines: IL-4, IL-5 and IL-10 (top panels) and typical T_{h1} cytokines: TNFα and IL-12 (bottom panels) was determined in BAL fluids by luminex bead array analysis as described in Materials and Methods. (B) Protein levels of homeostatic chemokines (CCL20, CXCL13, CCL21) in BAL fluid were measured by ELISA. Results are showed as the means ± SEMs, n= 4 mice per group. Data shown is representative of at least two separate experiments.

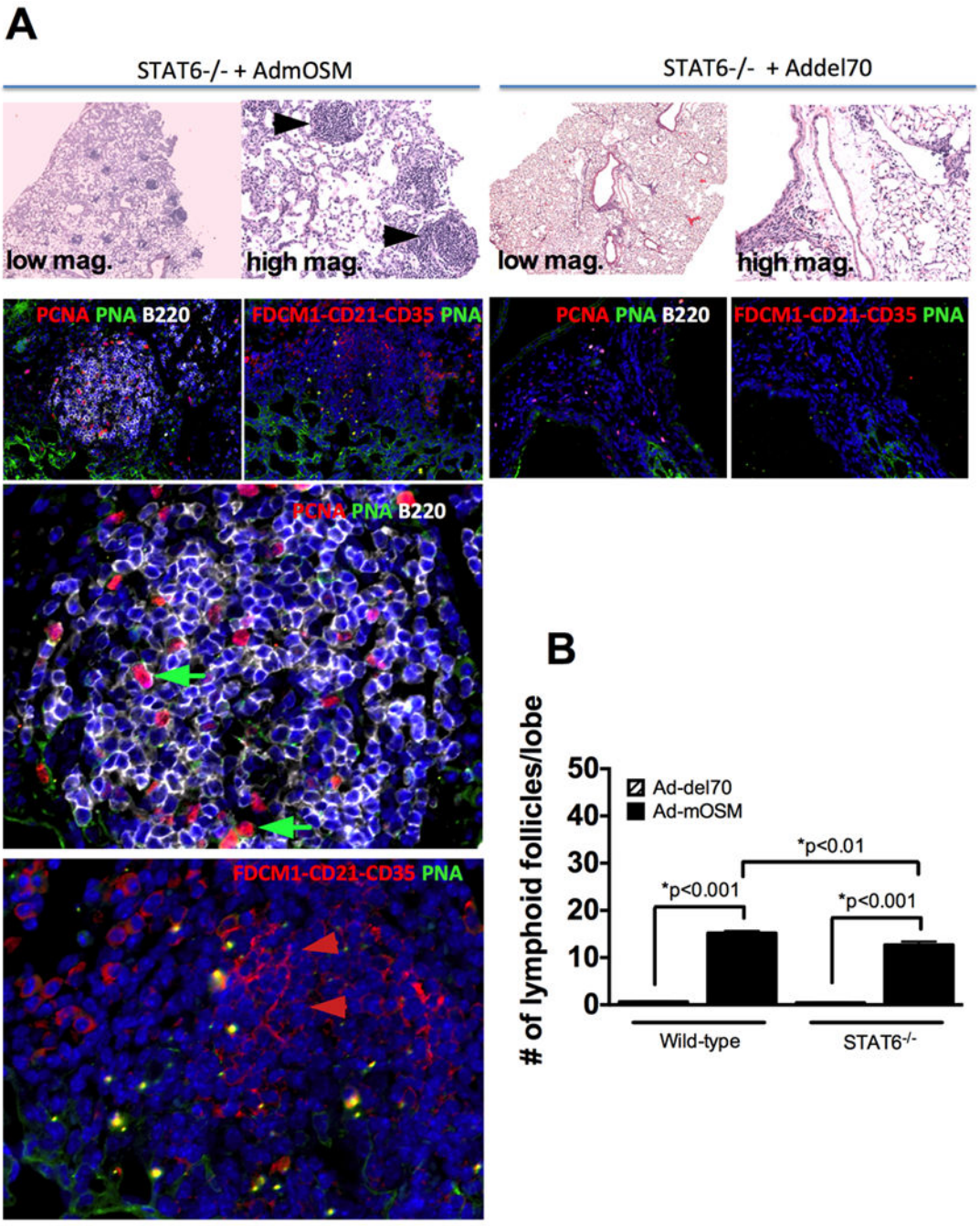

Figure 8. iBALT formation in wild-type and STAT6-deficient mice upon Ad-mOSM administration

C57Bl/6- STAT6-gene-deficient mice received Ad-del70 or Ad-mOSM, as described in Figure 1. 10% formalin-fixed lung tissues were examined for the presence of lymphocytic aggregates in H&E stained slides (A, top panels at 50× and 200× magnification). Complexity of iBALT structures was evaluated by staining for B220 (B cells, white surface stain) and PCNA (red nuclear stain) in (A) middle panels. Germinal center B cells were detected with peanut agglutinin (PNA, green surface stain, green arrows). Presence of FDC cells in the iBALT structures was assessed with a combination of antibodies against FDC

antigen, CD21, CD35 (red, red arrows). The two bottom staining images are magnifications of the 200× images from the Stat6-/- mice treated with Ad-mOSM. (B) Number of lymphoid follicles per lung lobe in C57BL/6- and Stat6-/- mice, infected with Ad-del70 or Ad-mOSM are shown. Results are presented as the means ± SEMs of at least five mice per group. Data shown is representative of at least two separate experiments.